1. INTRODUCTION

This report aims to explain in detail the research methods, process and results obtained in the development of a wing suitable for use in a remotely piloted vehicle (RPV). A secondary aim was to calculate the maximum payload that the RPV could carry. Performance analysis was conducted on three aerofoils, including tests in a closed loop wind tunnel, before a single aerofoil was selected to be taken forward for further investigation. This aerofoil was subjected to further performance analysis and structural calculations before the manufacture and flight tests. The flight test enabled comparisons to be undertaken to evaluate the actual load bearing capabilities of the RPV with the predicted results. This report will also highlight any errors observed and changes that would be made if this project were to be pursued further.

2. AEROFOIL SELECTION

Three aerofoils were chosen for their suitability for the project and were taken forward for wind tunnel testing. Data from the University of Illinois at Urbana–Champaign (UIUC) was used to aid in the selection process as this institution has conducted a series of aerofoil tests at low Reynolds numbers. The following aerofoils were selected for wind tunnel testing.

- S1223

The s1223 aerofoil is able to provide high lift at low Reynolds numbers. It has good stall characteristics which is useful when the aerofoil is being operated near the maximum lift coefficient, C_{LMAX} to achieve "low-speed flight requirements for loiter, cruise or landing." [1]

- SD7037

The SD7037 aerofoil is a modern, low Reynolds number aerofoil used in multitude of radio controlled aircraft. The aerofoil is often used for a similar purpose to our own so its performance is worth investigating further. It is overwhelmingly popular however it cannot guarantee optimum performance for a variety of sizes and weights of aircraft. [2]

- NACA 6409

The NACA 6409 aerofoil was chosen as it is a highly cambered aerofoil and provides maximum possible lift. It is also an aerofoil which is not specifically designed and used in remote control airplanes and small UAVs; this provided an interesting comparison between the aerofoils.

3. WIND TUNNEL TESTING

3.1 Wind tunnel aims

The wind tunnel was assumed to be located at sea level altitude due to the negligible temperature variation at 11m mean sea level. The wind tunnel was used to gain data on the performance of the three chosen aerofoils, the main values needed being lift and drag at various speeds and angles of attack. The aerofoils were tested at 10m/s and 20 m/s, and for a range of -5 to 14 degrees angle of attack. The angle of attack range was chosen to give the largest range possible for safe testing i.e. without damaging the wing. The aerofoils were tested in two degree increments to achieve a high level of accuracy without taking too much time.

3.2 Wind tunnel operation

In the wind tunnel air is pulled through the Venturi tube (high speed testing section) by a large fan, the air is then redirected around corners by large vanes angled at 45^{o} to the airflow. Air is continuously circulated through the duct in a closed loop tunnel. The vanes are necessary because the airflow produced by the fan is highly turbulent; these help settle this turbulence and redirect airflow. However, the flow is still far from laminar. Some drawbacks do come with using the wind tunnel as highlighted below. Although this was the case, it was still possible to obtain useful results and compare them to computer simulated results.

3.3 Wind tunnel errors

The following errors were observed during the testing of the aerofoils in the wind tunnel.

- ➢ The counterweight system, used to measure the lift force, caused a twist angle along the span of the wing. This effectively altered the lift characteristics of the section.
- ➢ The wing was initially referenced at 0^0 angle of attack by eye. Therefore an incorrect initial setup would result in a systematic error. Furthermore, variation in the initial angle used in different tests reduces the validity of any comparisons.

Figure 1. S1223 aerofoil in the wind tunnel during testing

- ➢ The closed loop wind tunnel contained sizeable objects in some sections. These were likely inducers of turbulence, decreasing the lift generated by the wings.
- ➢ The method by which the wing was supported introduced a degree of slip angle to the airflow. This reduced the magnitude of the velocity of the relative wind parallel to the chord line, reducing the lift generated by the wing.

The accumulation of these errors in the wind tunnel testing meant that the values produced were expected to be pessimistic and that the aerofoil would produce a higher lift during flight.

3.4 Wind tunnel results

As shown in Fig. 2 the wind tunnel results point to the NACA 6409 aerofoil performing best however there were some issues with the manufacture of the s1223 wind tunnel sample. Due to the very thin trailing edge a corner of the aerofoil broke off during the laminating process; it also suffered from twist during the testing. The graph of coefficient of lift for all three aerofoils was analysed alongside an external reference (fig. 3) for the s1223 and ultimately the s1223 aerofoil was chosen for further development.

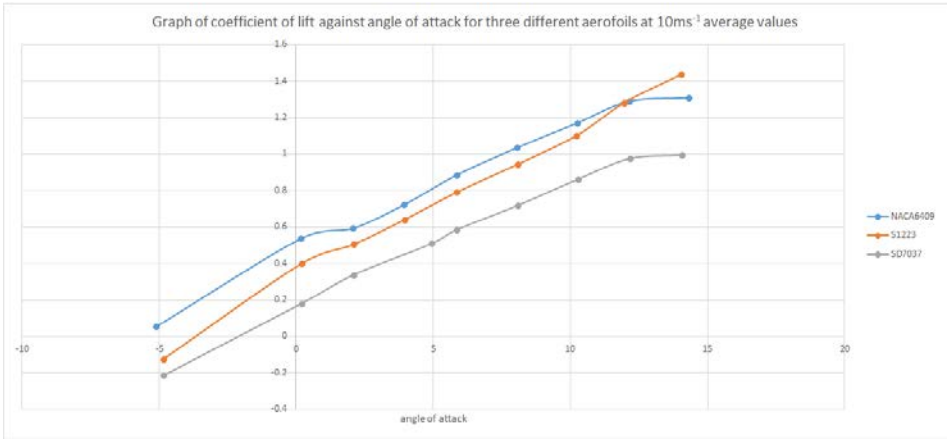

Figure 2. Graph of coefficient of lift vs. AOA for 3 aerofoils

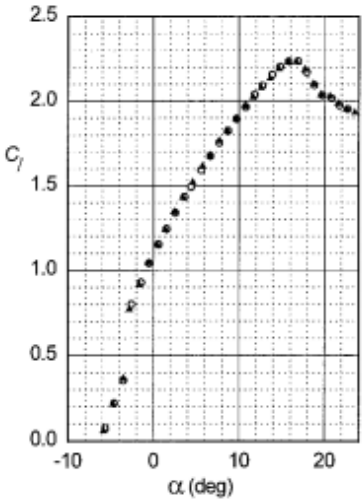

Figure 3. Coefficient of lift vs. AOA of s1223 [1]

4. ANALYSIS OF THE AEROFOIL IN JAVAFOIL

Using Javafoil, the lift and drag polars for the s1223 aerofoil were obtained. The lift curve slope and zero lift angle were obtained then it was then necessary to use the Lanchester-Prandtl corrections to convert the data for a wing of a given

aspect ratio. The lift curve generated by Javafoil is shown in figure 4. The value of the lift curve slope is a good approximation; however the very large zero lift angle of -13° is not accurate, and is vastly optimistic compared to the wind tunnel data. An extrapolation of the slope in the positive angle of attack region did not significantly alter this value.

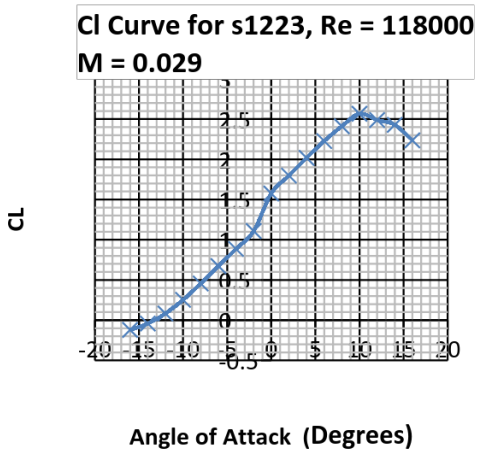

Therefore, in all further aerodynamic calculations, the values generated from the wind tunnel were used in order to predict the performance of the wing.

The lift and drag values were measured at obscure angles, such as 0.19°. A linear interpolation of the coefficients was undertaken in order to obtain data at integer values for α.

Wing drag is greater than aerofoil drag, due to the introduction of wing tip vortices. This value is known as induced drag, which is proportional to the square of the lift coefficient. For ease of manufacture a rectangular wing, with no wash out or wash in angle, was selected. This enabled standard value of the span efficiency factor, e, to be used. Where data did not exist, the linear relationship between aspect ratio and span efficiency allowed an accurate extrapolation for the values A = 2 and A = 12.

Figure 4. Lift curve slope for s122, per Javafoil

5. OPTIMISATION OF THE DESIGN

The wing parameters that could be altered were the span and chord length. The chord was constrained by the space on the aeroplane fuselage upon which to mount the wing, and was therefore set at the maximum possible length, 0.2m. Maximum span was constrained by weight, stability and structural factors.

5.1 Aspect Ratio Selection

The design of any wing is a compromise between aerodynamic and structural considerations. From a purely aerodynamic perspective, it would be advantageous to use the greatest possible aspect ratio. The Lanchester–Prandtl corrections determine that an increase in aspect ratio is accompanied by an increasing lift curve slope. Additionally, the induced drag coefficient is inversely proportional to aspect ratio. In order to finalise the configuration, it was therefore necessary to investigate structural constraints and wing loading.

Wing loading is defined as the weight of the aircraft divided by the planform area of the wing. Aircraft with low wing loadings are able to take off and land at lower speeds (or be able to take off with a greater load) [3]. These are desirable characteristics, as the model aircraft is to be thrown and will therefore encounter low speeds on launch. Furthermore, a design goal was to carry as much payload as possible. However, adverse characteristics include potential longitudinal static instability in gusty conditions. A low wing loading (high aspect ratio) configuration will have a steeper lift curve slope, as predicted by Lanchester-Prandtl. Therefore any gust altering the angle of attack will be accompanied by a greater change in lift coefficient, resulting in a bumpy ride that will place the wing structure under greater stress. [4] An analysis of forces on the airframe due to loading factors was undertaken in order to ensure the airframe was structurally stable under maximum stress.

5.2 Structural Analysis

Structural analysis is necessary to make sure the material used to create the wing would be able to support the load carried with a 2g loading factor. A 2g loading factor was used because an aircraft being subjected to a 60° angle of bank during a turn would experience a similar loading factor during flight. A worst case scenario was assumed whereby the load factor was treated as a point load at the wing tip. The material used for the wing was an expanded polystyrene floor insulation block, XFLOOR 300 from Cellecta insulation manufactures. However as the required specifications were not provided by the company, a match was found using the specifications that were provided on the company's

specification list and CES EduPack 2014 software. The closest match to XFLOOR300 was Expanded polystyrene (EPS) closed cell foam with a 0.02 specific gravity (based on styropor 20), This has a Flexural strength of 0.33-0.57MPa.

The structural calculations were based off the assumption that the total weight of the unloaded aircraft would be 0.975Kg. Our aircraft turned out to be 0.838Kg meaning that the calculations are not completely accurate. With the weight of the total aircraft being given at 0.838kg and our aim to carry 1kg payload this gives a total of 1.838kg. The wing length being tested was 2.4m with an aspect ratio of 12. However as the wing is loaded on the top of the fuselage, a loading diagram can be simplified due to the symmetry of the loading. Therefore we shall use a wing length of 1.2m and a chord of 0.2m to create a bending moment and shear stress diagram.

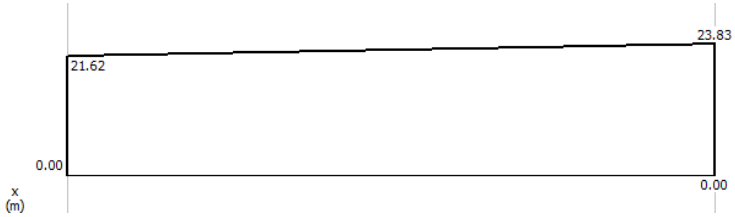

Figure 5. Shear diagram

From the shear of 23.83N and a bending moment of 27.27 Nm, a pressure can be worked out for a section of the wing 1% of the wingspan. This came out at 218 kPa which is comfortably within in the 330 KPa lower bending strength limit from the CES data.

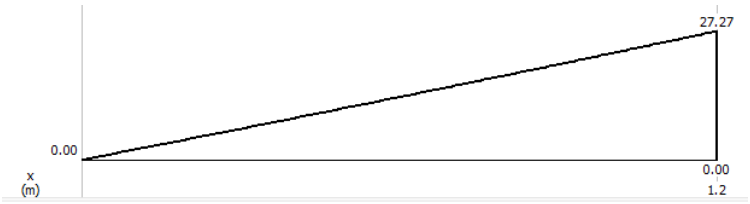

Figure 6. Moment diagram

5.3 Dihedral Angle Selection

Analysis of longitudinal stability in the event of gusting has been achieved; however during flight gusting has the capacity to affect the aircraft's lateral stability. A dihedral angle is designed to increase lateral stability by introducing a tendency to roll toward equilibrium, after being subjected to a small roll displacement.

The magnitude of dihedral angle is limited through additional characteristics; wings suffer from a degraded $\frac{Lift}{Weight}$ratio and decreased manoeuvrability. It is also worth noting that the UAV has a high wing mounting, and as such does not require as much dihedral as a low wing loading. This is because the dropped wing adopts a position of increased angle of attack to the relative wind. As a result, the greater lift force induces a stabilising moment, returning the aircraft to equilibrium. Due to time constraints on the project, the final chosen value of dihedral was in accordance to guidelines stated in *Civil Jet Aircraft Design* [5]. The recommended dihedral angle for conventional, unswept trapezoidal high wing is 0 - 1^{o}, and as a result a value of 1^{o} was selected.

5.4 Setting Angle Selection

For an aircraft to be in cruise conditions, two conditions have to be met: lift = weight and thrust = drag.
The lift = weight condition provides information regarding the velocity that must be achieved such that the lift generated by the aircraft can support its weight. Since lift is a function of angle of attack, altering the setting angle of the wing affects the required velocity as shown in figure 7.

Setting the wing at an angle with respect to the longitudinal axis of the aircraft allows it to operate at a higher angle of attack. It is therefore able to generate greater lift. Since lift $\propto$ velocity^2, to satisfy the lift = weight cruise condition, the velocity of the aircraft decreases. Flying the aircraft at the same velocity would enable it to carry a greater payload. As a result, it was desirable to introduce a moderate setting angle into the design of the UAV. In order to satisfy the thrust = drag condition, a plot of thrust required against thrust available was constructed, as shown in Figure 8.

The thrust = drag requirement was plotted for setting angles of 2, 3 and 4 degrees. Extracting the values where the two curves intersected; it was possible to construct a plot of the predicted cruise conditions of the UAV. The values for a setting angle of 2 are displayed in Figure 9.

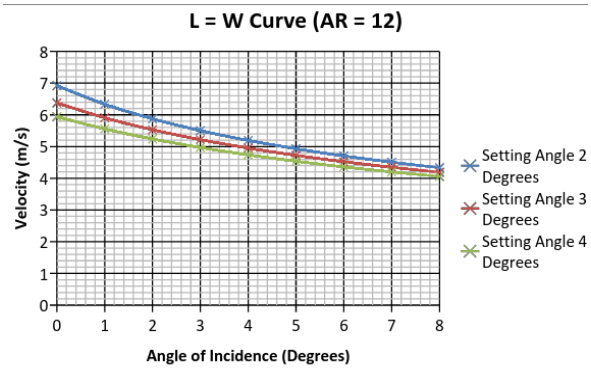

Figure 7. L=W Curve at aspect ratio 12

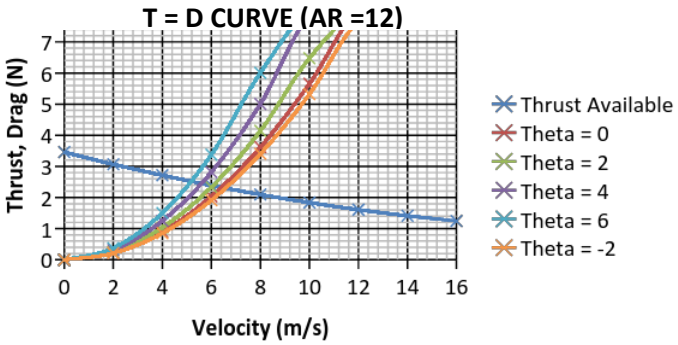

Figure 8. T = D Curve at aspect ratio 12

After obtaining plots for the cruise conditions for the three setting angles, a value of 2^0 was selected. This is because this configuration would have to be flown at a greater velocity for the straight and level flight criteria to be met. Increasing the cruise velocity was desirable, so that the UAV would fly well in a headwind.

5.5 Aileron Selection

It was decided that the wing would have ailerons attached both to increase the coefficient of lift without affecting the cruise characteristics and to increase manoeuvrability. Ailerons were chosen due to the fact that they are easy to manufacture, are effective and are cheap. The ailerons are used in tandem to cause a rolling motion which causes a turn; if the right aileron is deflected upwards the left aileron will be deflected downwards. [6] The roll is caused by the difference in lift between the wings; the lift is decreased when an aileron is deflected up causing the wing to drop and the plane to roll to that side. [7] The ailerons were cut at the wingtip of each wing as the reaction time decreases and effectiveness of the aileron increases the further they are from the centre of the plane. [8] Below are the calculations to show the choice of size of the ailerons.

The smallest area ratio was used to create the largest ailerons, which in turn increases the effect of the ailerons. It was chosen that the "barn door" style ailerons would be implemented, mainly due to the manufacturing restrictions – the trailing edge of the aerofoil was extremely fine and susceptible to breaking. The main design factor considered was the area ratio, which is defined as $\frac{Planform\ Area}{Aileron\ Area}$. In order to maximise aileron effectiveness, the largest allowable size was used. The final area ratio selection was 53.3. A small length to width ratio of 10 was selected to create a stronger set of ailerons less susceptible to damage and twist.

Planform area = 20 x 240 = 4800 cm^2

Area ratio = 50 – 70

Aileron width to length ratio = 10 – 22

For ease of manufacture the dimensions of the ailerons were 30 cm x 3 cm which meant the ailerons had our desired ratios.

$$\text{Area ratio} = \frac{Planform\ Area}{Aileron\ Area} = \frac{4800}{90} = 53.33$$

$$\text{Length to width ratio} = \frac{Aileron\ Width}{Aileron\ Length} = \frac{30}{3} = 10$$

5.6 Final design layout

- S1223 aerofoil with a wing aspect ratio of 12
- Setting angle 2° and dihedral angle 1°
- Ailerons at wing tips with dimensions 30 x 3 cm

6. CRUISE CONDITIONS AND MAXIMUM PAYLOAD PREDICTIONS

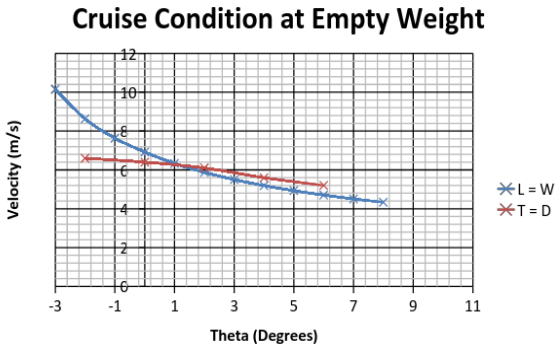

Figure 9. Cruise condition unloaded

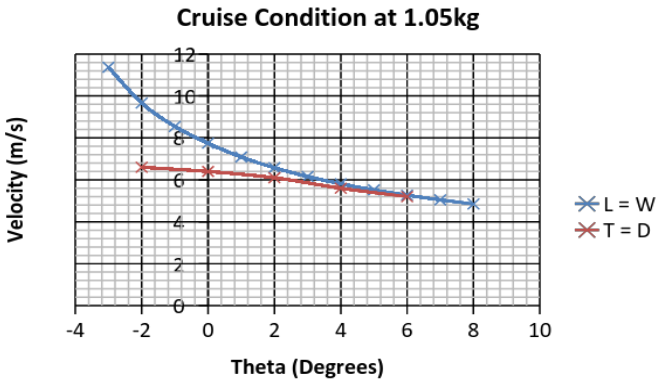

Figure 10. Cruise condition loaded

The total mass of the UAV wing and body combination was 0.838kg. The configuration of the aircraft in this state is predicted in figure 9. The UAV will adopt an angle of incidence of approximately 2° and must maintain a velocity of 6m/s. To calculate the maximum payload, the mass of the aircraft was increased until the T=D and L=W curves would no longer meet. This signifies that the cruise condition cannot be met. The maximum weight where the UAV is able to sustain level flight, as predicted through the wind tunnel test, is shown in figure 10. Increasing the weight beyond 1.05kg resulted in a divergence of the two curves. A maximum weight of 1.05kg represents a maximum payload of 0.212 kg.

7. MANUFACTURING

7.1 Manufacturing process

The main components of the aerofoil were manufactured as described in the "Wings Week Aileron Tutorial." [9] To produce the desired dihedral angle, a small length of steel bar about 10cm long was bent into shape; this was simply done by securing one end in a vice and tapping it with a mallet. Once the wings were assembled together, an offcut from the original hot wire cutting the same width of the fuselage was used to produce a base block for the wings to sit upon. This block was shimmed along upper port and starboard edges in order to accommodate the dihedral angle of the wings, and then shimmed along the lower forward edge to produce the desired incidence angle of the wing. This block was then assembled to the wings and the whole assembly then fastened to the fuselage before flight.

7.2 Manufacturing errors

There were a reasonable amount of errors associated with the manufacture, as listed below.

- The recommended position for the servos was at the quarter chord, however due to the carbon fibre spar at that location the servos were positioned slightly aft of the quarter chord. Due to the thickness of the wing at that position it was not possible to house the servos flush with the surface of the wing. This resulted in an extrusion of a few millimetres as shown in Figure 11.

- ➢ A small part of a trailing edge corner of one of the ailerons snapped off. Once covered in solar film the broken corner was hard to see as the trailing edge is so fine, however it could still have affected the flight test results.
- ➢ The aerofoil did not have a smooth surface due to certain components such as the servos and base block having clear tape attached at multiple points.
- ➢ As our ailerons cut from our aerofoil are so thin, during flight they may experience bending. This may cause our roll movement to be less reactive at higher speeds.
- ➢ The extrusions and the position of the servos themselves may be slightly different on each wing causing the moment forces acting upon each wing will be different.

8. FLIGHT TEST

During the flight test, the UAV was loaded with payload by strapping it to the underside of the fuselage. The aircraft was able to sustain level flight carrying weights of 0.6 kg and 0.8kg. This is higher than the predicted maximum payload of 0.212kg. The reason for the difference in theoretical and actual results is based largely on the use of wind tunnel data for predictions. For the reasons described on page 2 of this report, the losses in the wind tunnel due to turbulence gave rather pessimistic values of the lift and drag generated by the wing. Note that CL_0 as calculated for the wind tunnel was 0.4 compared to the Javafoil value 1.35. These two methods of obtaining lift values produced very different predictions for maximum payload; with reference to Part B Javafoil predicted a maximum payload of 1.538 Kg compared to the wind tunnel estimation of 0.212 Kg.

9. CONCLUSION

This report has outlined a rudimentary approach to designing a suitable wing for a UAV. Selection of an effective low Reynolds number aerofoil, large aspect ratio and moderate setting angle enhanced the lifting capabilities. Moreover, inclusion of dihedral angles and ailerons increased the lateral stability and manoeuvrability of the aircraft. Justification for each design decision has been made, and ultimately the final design achieved in carrying a greater than predicted payload.

The use of both wind tunnel testing and Javafoil were explored, and their inaccuracies noted. Javafoil showed a difficulty in modelling the characteristics of the s1223 aerofoil, as the lift and drag values were extremely optimistic. This presented a difficulty in modelling the cruise condition of the aircraft, and as such wind tunnel data was used. An acquired knowledge of the inefficiencies of the wind tunnel was used to explain the exceptional performance of the UAV, in terms of its lifting capability.

An interesting note on which to end this report is the influence of C_{L0} on the maximum payload predictions. C_{L0} was -4.7^0 and -13^0 for the wind tunnel and Javafoil respectively. The value published by UIUC (figure 3) shows -6^0, and should be treated as the most accurate prediction. The maximum predicted payloads were 0.212kg and 1.538kg, whereas in flight test this was 0.8kg. If the wind tunnel results were corrected, and C_{L0} altered to be closer to published data, the payload prediction would have been more accurate.

References

[1] Michael S. Selig and James J. Guglielmo (1997) *High-Lift Low Reynolds Number Airfoil Design*. Available from: http://m-selig.ae.illinois.edu/pubs/GuglielmoSelig-1997-JofAC-S1223.pdf [Last accessed 22 March 2015]

[2] (2015) *Systematic Airfoil Design Studies at Low Reynolds Numbers*. Available from: http://pawan.mae.ncsu.edu/~ashok/pubs/ND_low_Re_conf_paper.pdf [Accessed 22 March 2015].

[3] Science Learn. (2011). *Wing Loading.* Available: http://sciencelearn.org.nz/Contexts/Flight/Science-Ideas-and-Concepts/Wing-loading. [Last accessed 20 March 2015]

[4] Anderson, J. (2012). Airfoils, Wings and Other Aerodynamic Shapes. In: *Introduction to Flight*. 7th ed. New York: McGraw-Hill. 372-378. [Last accessed 7th March 2015].

[5] Jenkinson, L.R.. (1999). Wing Layout. In: *Civil Jet Aircraft Design*. Oxford: Butterworth-Heinemann. p117. [Last accessed 7th March 2015].

[6] Benson, T. (2014). *Ailerons.* Available: http://www.grc.nasa.gov/WWW/k-12/airplane/alr.html. Last accessed 20.02.2015.

[7] Ali, J. (2012). S*teering an Aircraft: Use Ailerons for Lateral Control in Planes.* Available: http://www.decodedscience.com/steering-an-aircraft-use-ailerons-for-lateral-control-in-planes/11727. Last accessed 20.02.2015.

[8] Abbot and Von Doenhoff. (1959). High-lift devices. In: *Theory of wing sections*. New York: McGraw-Hill. 190-207.

[9] (2015). *Aileron tutorial.* Available: https://blackboard.uwe.ac.uk/bbcswebdav/pid-4063620-dt-content-rid-6956807_2/courses/UFMFY6-30-2_14sep_fr_jun15_1/Aileron%20Tutorial.pdf. Last accessed 20th March 2015.